Atmos. Chem. Phys. Discuss., 14, 26689–26719, 2014
www.atmos-chem-phys-discuss.net/14/26689/2014/
doi:10.5194/acpd-14-26689-2014
© Author(s) 2014. CC Attribution 3.0 License.

Atmospheric Chemistry and Physics Discussions
Open Access

This discussion paper is/has been under review for the journal Atmospheric Chemistry and Physics (ACP). Please refer to the corresponding final paper in ACP if available.

Modulation of Saharan dust export by the North African dipole

S. Rodríguez[1], E. Cuevas[1], J. M. Prospero[2], A. Alastuey[3], X. Querol[3], J. López-Solano[1], M. I. García[1,4], and S. Alonso-Pérez[1,3,5]

[1]Izaña Atmospheric Research Centre, AEMET, Joint Research Unit to CSIC "studies on atmospheric pollution", 38071, Santa Cruz de Tenerife, Canary Islands, Spain
[2]Rosenstiel School of Marine and Atmospheric Science, University of Miami, Miami, Florida, USA
[3]Institute of Environmental Assessment and Water Research, CSIC, Barcelona, Spain
[4]Department of Chemistry (T.U. Analytical Chemistry), Faculty of Science, University of La Laguna, Tenerife, Spain
[5]European University of the Canaries, Laureate International Universities, La Orotava, Tenerife, Spain

Received: 16 September 2014 – Accepted: 1 October 2014 – Published: 24 October 2014

Correspondence to: S. Rodríguez (srodriguezg@aemet.es)

Published by Copernicus Publications on behalf of the European Geosciences Union.

CC BY

Abstract

Desert dust aerosols influence air quality and climate on a global scale, including radiative forcing, cloud properties and carbon dioxide modulation through ocean fertilisation. North Africa is the largest and most active dust source worldwide; however, the mechanisms modulating year-to-year variability in Saharan dust export in summer remains unclear. In this season, enhanced dust mobilization in the hyper-arid Sahara results in maximum dust impacts throughout the North Atlantic. The objective of this study is to identify the relationship between the long term interannual variability in Saharan dust export in summer and large scale meteorology in western North Africa. We address this issue by analysing ~25 yr (1987–2012) dust concentrations at the high altitude Izaña observatory (2373 m a.s.l.) in Tenerife Island, satellite and meteorological reanalysis data. Because in summer Saharan dust export occurs at altitudes 1–5 km, we paid special attention to the summer meteorological scenario in the 700 hPa standard level, characterised by a high over the subtropical Sahara and lower geopotential heights over the tropics; we measured the intensity of this low-high dipole like pattern in terms of the North AFrican Dipole Index (NAFDI): the difference of the 700 hPa geopotential heights anomalies averaged over central Morocco (subtropic) and over Bamako region (tropic). The correlations we found between the 1987–2012 NAFDI with dust at Izaña, satellite dust observations and meteorological re-analysis data, indicates that increase in the NAFDI (i) results in higher wind speeds at the north of the Inter-Tropical Convergence Zone which enhances dust export over the subtropical North Atlantic, (ii) influences on the size distribution of exported dust particles, increasing the load of coarse dust and (iii) are associated with higher rainfall over tropical North Africa and the Sahel. Because of the North African dipole modulation, inter-annual variability in Saharan dust export is correlated with monsoon rainfall in the Sahel. High values of the NAFDI enhance dust export at subtropical latitudes. Our results suggest that long term variability in Saharan dust export may be influenced by global oscillations in the

CC BY

climate of the tropics and subtropics and that this may have influenced dust transport pathways in the last decades.

1 Introduction

Desert dust aerosols influence global climate by scattering and absorbing radiation (Forster et al., 2007), influencing rainfall (Creamean et al., 2013), and also by modulating ocean–atmosphere CO_2 exchange through the deposition of dust which supplies iron, a micronutrient for marine biota (Jickells et al., 2005). Ice core records show increased dust activity during glacial periods when CO_2 was low (Martínez-García et al., 2009). Dense dust hazes often occur between tropical and mid-latitudes over the North Atlantic (Tanaka and Chiba, 2006), with implications also on air quality (Rodríguez et al., 2001; Pérez et al., 2008; Mallone et al., 2011; Díaz et al., 2012; Prospero et al., 2014). Consequently, there is considerable interest in climate variability, the global distribution of dust (Adams et al., 2012; Ginoux et al., 2012) and dust microphysical properties including particle size which modulates dust impacts (Mahowald et al., 2014) (e.g. the interaction with radiation (Otto et al., 2007), iron solubility and supply to the ocean (Baker and Jickells, 2006), its role as cloud and ice nuclei (Welti et al., 2009), and health effects due to dust exposure (Pérez et al., 2008, 2014; Mallone et al., 2011; Díaz et al., 2012)). During atmospheric transport, dust is removed by precipitation and by dry deposition, the latter a process that is strongly size dependent. Dust size variability is observed over time scales of individual dust events (∼ days) (Ryder et al., 2013) and in ice cores, over thousands of years, linked to changes in wind speeds, transport pathways and dust sources attributed to climate variability (Delmonte et al., 2004).

North Africa is the largest and most active dust source in the world (Ginoux et al., 2004, 2012; Huneeus et al., 2011). Dust mobilization experiences a marked seasonality. In winter, sources located in southern Sahara and the Sahel ($< 20^\circ$ N) are especially active linked to north-easterly dry (Harmattan-trade) winds which prompt dust

ACPD
14, 26689–26719, 2014

export across the North African tropical coast (< 15° N) (Engelstaedter and Washington, 2007; Haywood et al., 2008; Menut et al., 2009; Marticorena et al., 2010). In summer, the north-east trade winds and the Inter-Tropical Convergence Zone (ITCZ) shift northward, enhancing emissions from Saharan sources and increasing dust export at subtropical latitudes (20–30° N), concurrently the shift in the monsoon rainfall to southern Sahel tends to decrease Sahelian dust emissions (Engelstaedter and Washington, 2007; Knippertz and Todd, 2010; Ashpole and Washington, 2013, and references therein).

There is a major scientific interest in understanding the links between long term variability in North African dust export and climate. Dust sources in part of the Sahel have a hydrological nature (Ginoux et al., 2012); their emissions are affected by the summer variability in rainfalls and also by the North Atlantic Oscillation in winter, and this has had consequences on dust impacts on the tropical North Atlantic detected during, at least, four decades (Prospero and Lamb, 2003; Chiapello et al., 2005). In addition, the increase in commercial agriculture over the last two centuries coupled with droughts has had an impact on Sahelian dust emissions (Mulitza et al., 2010). In contrast the Sahara is a hyper-arid environment (< 200 mm yr^{-1}) where natural non hydrological dust sources (i.e. not associated with annual hydrological cycles) prevail (Ginoux et al., 2012), and dust emission variability is mainly controlled by winds (Engelstaedter and Washington, 2007; Ridley et al., 2014). Conceptual model explaining interannual variability in Saharan dust export have been proposed for the winter (e.g. North Atlantic Oscillation by Ginoux et al., 2004; Chiapello et al., 2005), but not for summertime when the highest dust emissions occur in North Africa due to the enhanced activation of the Saharan sources (Prospero and Lamb, 2003; Ginoux et al., 2004; Chiapello et al., 2005; Tanaka and Chiba, 2006; Engelstaedter and Washington, 2007; Mulitza et al., 2010; Knippertz and Todd, 2012; Ridley et al., 2014).

Starting in 1987 we have measured aerosols at the Izaña – Global Atmospheric Watch (GAW) – World Meteorological Organization (WMO) – high-mountain observatory (28° 18′ N, 16° 29′ E, 2373 m a.s.l.) on Tenerife Island, which frequently lies under

ACPD
14, 26689–26719, 2014

cc BY

the main path of Saharan dust outbreaks. At night, when mountain upslope winds cease, Izaña is located in the free troposphere. In summer, Izaña is frequently within the dust-laden Saharan Air Layer (SAL) which in this season is typically located at altitudes between 1 to 5 km a.s.l. (Adams et al., 2012; Nicholson, 2013; Tsamalis et al., 2013). Here we report on long term measurements of summertime concentrations of total dust ($dust_T$) (1987–2012) and of dust particles < 2.5 µm ($dust_{2.5}$) (2002–2012). Our 25 years observation evidence that there is a significant interannual variability in Saharan dust export in summer. Our research focuses on one key question: *what is the relationship between long term inter-annual variability in Saharan dust export in summer and large scale meteorology in North Africa?* For addressing this issue we also used the UV Aerosol Index determined by the Total Ozone Mapping Spectrometer and Ozone Monitor Instrument satellite-borne spectrometers (Herman et al., 1997) for studying long-term and interannual spatial distribution of dust and gridded meteorological National Center for Environmental Prediction/National Center for Atmospheric Research (NCEP/NCAR) re-analysis data (Kalnay et al., 1996) for studying the variability of large scale meteorological processes.

In this article, we first perform a brief description of the typical meteorological scenario in western North Africa in the summertime. Then, the concept of the North African dipole is introduced as an approach to characterize how variability in large scale meteorology may influence Saharan dust export. We then assessed how the long term variability in the intensity of the North African dipole has influenced long term Saharan dust export to the free troposphere during 25 years and particle size distribution during 11 years. Finally, we assess whether the North African dipole index proposed here can be used to connect Saharan dust export with climate variability. Here we present connections between dust export and large scale meteorology; further studies will be necessary for understanding the involved meteorological and dust processes.

ACPD
14, 26689–26719, 2014

CC BY

2 Methods

2.1 In-situ dust measurements

We used in-situ dust concentrations data recorded between 1987 and 2012 at Izaña observatory. Here we present a brief description of the methods. Technical details are included in the Supplement.

Dust concentrations were obtained by chemical analysis of aerosol samples collected on filter at the flow rate of $30\,m^3\,h^{-1}$. Here we report on dust concentrations in two size fractions: concentrations of total dust ($dust_T$) from 1987 to 2012 and of dust particles with an aerodynamic diameter $\leq 2.5\,\mu m$ ($dust_{2.5}$) from 2002 to 2012 (Rodríguez et al., 2011).

Dust concentrations were also calculated with a secondary complementary method based on number size distributions measurements (0.5 to 20 µm) performed with an Optical Particle Counter and an Aerodynamic Particle Sizer. These data were used for determining the aerosol volume concentrations and convert then to bulk aerosol mass concentrations using standard methods (Rodríguez et al., 2012). The good agreement (high linearity and low mean bias, 3–8 %) between these two methods (based on chemical analysis and on size distributions) is due to the very low aerosol volume concentrations in the free troposphere during no dust events (typically < 1 to $3\,\mu g\,m^{-3}$; Rodríguez et al., 2009) and to the fact that the aerosol volume concentrations during dust events are by far dominated by dust, as evidenced by the chemical analysis (Rodríguez et al., 2011) and the ochre color of the aerosol samples.

These two dust databases (based on chemical and on size distribution methods) were used to assess the consistency of the observed year-to-year variability of dust. During the whole measurement period (25 July 1987–31 December 2012, excluding the none-measurement period 11 October 1999–13 February 2002), dust concentrations records are available for 7348 days, which lead to a data availability of 87 %. This long term dust concentration record is among the longest in the world (after Barbados – started in 1965, Miami – 1972 and American Samoa – 1983) and probably the longest

ACPD
14, 26689–26719, 2014

dust record in several size fractions downwind of a dust large source (Rodríguez et al., 2012).

2.2 Satellite dust observations

We used UV Aerosol Index (AI) data from the Total Ozone Mapping Spectrometer – TOMS – (1979–2001) and from the Ozone Monitor Instrument – OMI – (2005–2012) spectrometers onboard the satellites Nimbus 7 (TOMS 1979–1993), Earth Probe (TOMS 1996–2001) and Aura (OMI 2005–2012) for studying the spatial and temporal variability of dust. Because of the UV absorption by some minerals (e.g. hematite, goethite), AI has been widely used in dust studies. This is a semi-quantitative parameter; AI values >1 are considered representative of an important dust load and the frequency of daily AI values >1 has been used for dust climatology (Prospero et al., 2002). In North Africa, the AI signal at the north of the summer tropical rain band is due to dust, whereas biomass burning aerosols transported from South Africa contribute to AI signal at the south of the tropical rain band (Prospero et al., 2002). We only analyzed and interpreted the variability in the frequency of daily AI >1 at the north of the summer tropical rain band. The following data were used:

- Level 3 TOMS data of the period 1979–2001. TOMS Data for the period 2002–2005 were not used due to calibration problems (http://disc.sci.gsfc.nasa.gov/guides/legacy-guides/tomsl3_dataset.gd.shtml).

- Level 3 OMI data of the period 2005–2012. Although this instrument has experienced the so called "row anomalies" since 2007 (http://www.knmi.nl/omi/research/product/rowanomaly-background.php), the affected data is not included in the level 3 datasets (http://disc.sci.gsfc.nasa.gov/Aura/data-holdings/OMI/index.shtml#info).

Level 3 daily AI data of TOMS and OMI of summer (August) were downloaded from the Giovanni online data system of the NASA Goddard Earth Sciences Data and Infor-

ACPD
14, 26689–26719, 2014

cc BY

mation Services Centre (GES DISC) (http://disc.sci.gsfc.nasa.gov/). The consistency of the TOMS and OMI AI data set has already been shown (Li et al., 2009).

2.3 Meteorological reanalysis data

We used gridded meteorological National Center for Environmental Prediction/National Center for Atmospheric Research (NCEP/NCAR) re-analysis data (Kalnay et al., 1996) for studying relationship between dust variability and large scale meteorological processes in summer (August). This analysis included geopotential heights, winds and rains used in Eq. (1) (shown below) and Fig. 2.

NCEP data were also used for determining 10 day back-trajectories calculated with the HYbrid Single-Particle Lagrangian Integrated Trajectory (HYSPLIT) model (Draxler and Rolph, 2013) developed by the NOAA Air Resources Laboratory. Back-trajectories were used for assessing the consistency of our interpretations; more specifically we assessed whether the regions that seem to play an important influence on dust mobilization were potential dust sources and/or within the transport pathways of the dust recorded at Izaña. For the sake of brevity the trajectory analysis is included in the Supplement.

2.4 Summer dust season

At Izaña, the summer dust season (impacts of the SAL) typically starts in the second half of July and ends at the beginning of September. The maximum frequency of dust events occurs in August (52 % of the August-days as average; Supplement). This month is of high interest given that (i) the ITCZ is shifted to the North and consequently (ii) the SAL is exported at the northern most latitude (as evidence the highest frequency of dust impacts at Izaña; Tsamalis et al., 2013) and the maximum rainfall occurs in tropical North Africa (Nicholson, 2009). For this reason, we used the August dust averages for studying summer long term dust evolution in the boreal subtropics (Fig. 1a). The study of the central month (August) of the summer dust season (exclud-

CC BY

ing July and September) allows characterizing long term evolution in terms of intensity of dust export, avoiding the variability that could be linked to (i) shifts in the beginning (July) or end (September) dates of the dust season or (ii) variability in the location of the ITCZ from July to September. Our data analysis shows that the July to September dust average is dominated by the dust events occurring in August (see details in the Supplement). In August 1987–2012, daily dust data were available during 699 days, i.e. a data availability of 97 % (excluding the no measurements period 11 October 1999–1913 February 2002). In this study we analyse 1987–2012 time series of dust concentration averaged in August. We refer to August as summer.

3 North African summer meteorological scenario

Meteorological scenario throughout western North Africa is influenced by the high pressures typical of the subtropical deserts and the so-called western African monsoon (Lafore et al., 2010). Additionally, the formation of the summer Saharan heat low (Lavaysse et al., 2009) in central western Sahara has also implications on meteorological processes, not only related to the development of the wet western African monsoon season in tropical North Africa (Lafore et al., 2010), but also on mobilization, upward transport and export of dust to the North Atlantic at subtropical latitudes (Jones et al., 2003; Flamant et al., 2007; Knippertz and Todd, 2010).

In summer, the vertical structure of the atmosphere over the Sahara is characterized by the Saharan heat low at low levels (surface to 925 Pa standard level at $\sim 20^{\circ}$ N) with a confluence of surface “northern dry desert Harmattan” and “southern humid monsoon” winds at its southern margin (Nicholson, 2013) in the so-called ITCZ, which in central western Sahara occurs between 18–20° N (Lafore et al., 2010; Pospichal et al., 2010; ITCZ also known as Inter-Tropical-Discontinuity ITD). Monsoon rainfalls occur at southern latitudes ($< 15^{\circ}$ N), in a region we will refer as rain band (Nicholson, 2009). The Saharan heat low, as a shallow hot depression, enhances subsidence processes due to compensatory downward movement in upper levels (Spengler and Smith, 2008;

ACPD
14, 26689–26719, 2014

CC BY

Canut et al., 2010). The African Easterly Jet (AEJ) forms at altitude between 2 and 6 km between 15 and 20° N due to the thermal wind in the baroclinic zone between the "northern hot desert air" and the "cool monsoonal southern airflow" (Nicholson, 2009, 2013).

Emissions, upward transport and export of dust to the North Atlantic occur in this summer scenario. Dust emission processes occur in a range of scales (Knippertz and Todd, 2012) from (i) synoptic scale (e.g. Harmattan-trade winds, African easterly waves; Jones et al., 2003; Knippertz and Todd, 2010), through (ii) strong winds, convergence and high turbulence associated to the ITCZ (Flamant et al., 2007; Ashpole and Washington, 2013), low-level jets (Knippertz, 2008; Fiedler et al., 2013; Cowie et al., 2014) and cold pools of mesoscale dry convective systems (particularly over the Sahel; Engelstaedter and Washington, 2007; Lavaysse et al., 2010a, and references therein) including "haboob" storms (Marsham et al., 2008; Cowie et al., 2014), to (iii) microscale dust devils and dusty plumes (Allen and Washington, 2013). As a consequence of convergence processes close to the ITCZ (Ashpole and Washington, 2013) and because of the convective boundary layer, huge amounts of dust are lifted up to ∼ 5 km altitude (Cuesta et al., 2009; Guirado et al., 2014). The easterly subtropical circulation linked to the North African anticyclone typically present at the altitude of the 700 hPa level and aloft (Font-Tullot, 1950), coupled with the divergence linked to the Saharan heat low, and the AEJ (Lavaysse et al., 2010b) expands this dry dusty air mass over the North Atlantic free troposphere resulting in the previously described SAL (Prospero and Carlson, 1972; Tsamalis et al., 2013). Near the North African coast, the summer SAL is found at altitudes between 1 and 5 km (Karyampudi et al., 1999; Immler and Schrems, 2003; Tsamalis et al., 2013; Andrey et al., 2014) due to the westward dust export occurs above the so-called "Atlantic inflow", a layer of cool and stable sea-breeze like inflow present along the subtropical North African coast (Lafore et al., 2010).

This brief description illustrates how the presence of the dusty SAL over the North Atlantic is the net result of a set of complex and coupled processes which occur in a wide range of scales and which may also involve (i) feedback mechanisms (e.g. radiative,

ACPD
14, 26689–26719, 2014

CC BY

cloud and rain processes triggered by dust; Lau et al., 2009), (ii) interconnections between processes (e.g. influence of the AEJ-convection-monsoon connections on dust described by Hosseinpour and Wilcox, 2014), (iii) variability in dust emissions due to meteorologically driven variability in soil features (Prospero and Lamb, 2003) and (iv) dust microphysical processes (e.g. size dependent deposition and cloud and radiation interactions; Mahowald et al., 2014).

4 Results and discussion

4.1 The North African dipole

We aim to find a simple conceptual model for linking long term variability in Saharan dust export with variability in the large scale meteorology in western North Africa. Because summer dust export occurs between 1 and 5 km altitude (Prospero and Carlson, 1972; Immler and Schrems, 2003; Tsamalis et al., 2013; Ben-Ami et al., 2009), with a frequent maximum dust loads between 2 and 3 km (Tesche et al., 2009; Cuevas et al., 2014), we paid special attention to the 700 hPa standard level (Nicholson, 2013). The summer mean height of the 700 hPa geopotential field through western North Africa exhibits a strong northward gradient (see Supplement). Because it resembles a dipole, we refer to this pattern as North AFrican Dipole (NAFD), formed by a high over subtropical Sahara (27–32° N over Algeria; Font-Tullot, 1950) and lower geopotential heights over tropical North Africa (< 15° N) at 700 hPa. We measured the intensity of this low-high dipole like pattern in terms of the NAFD Index (NAFDI), defined as the difference of the anomalies of the 700 hPa geopotential height averaged over central Morocco (30–32° N, 5–7° W) and over Bamako region in Mali (10–13 ° N, 6–8 ° W):

$$\mathrm{NAFDI} = \frac{1}{10}\left(\left(\Phi^{y}_{\mathrm{Mo}} - \langle\Phi\rangle_{\mathrm{Mo}}\right) - \left(\Phi^{y}_{\mathrm{Ba}} - \langle\Phi\rangle_{\mathrm{Ba}}\right)\right) \quad (1)$$

where,

ACPD
14, 26689–26719, 2014

CC BY

- Φ^{y}_{Mo} is the mean geopotential height at 700 hPa averaged in central Morocco region (30–32° N, 5–7° W) in August of year "*y*".

- $\langle\Phi\rangle_{\mathrm{Mo}}$ is the mean geopotential height at 700 hPa averaged in central Morocco region (30–32° N, 5–7° W) averaged in August months from 1948 to 2012.

- Φ^{y}_{Ba} is the mean geopotential height at 700 hPa averaged in Bamako region (10–13° N, 6–8° W) in August of year "*y*".

- $\langle\Phi\rangle_{\mathrm{Ba}}$ is the mean geopotential height at 700 hPa averaged in Bamako region (10–13° N, 6–8° W) averaged in all August months from 1948 to 2012.

The NAFDI (Eq. 1) is a measure of the inter-annual variability of the dipole intensity and, because of its relationship with the geopotential gradient, it is related with the intensity of the geostrophic North African outflow.

The NAFD is illustrated in Fig. 2a with the mean 700 hPa geopotential height field during summers of low and of high NAFDI. The core of the northern Saharan anticyclone reinforces over the western Atlas Mountains (~ 30° N) in high NAFDI summers (Fig. 2a2), whereas it weakens and shifts southward to central Algeria (~ 28° N) in low NAFDI summers (Fig. 2a1). Conversely, at the tropical latitude of Bamako (~ 12° N) geopotentials heights are higher during low NAFDI summers (Fig. 2a1) than during high NAFDI summers (Fig. 2a2). The variability in the NAFDI has implications on other standard levels (Supplement).

4.2 Long term variability of Saharan dust export

At Izaña we observe a strong interannual variability in dust concentrations (Fig. 1a). In low dust years – 1987, 1997, 2006 and 2007 – mean concentrations were within the range 17–30 µg m^{-3}; in high dust years – 1988, 2008, 2010 and 2012 – the range was 100–140 µg m^{-3}. We associate this variability to the spatial variability of meteorological conditions over North Africa specifically, to the NAFD. The high value of the Pearson

CC BY

correlation coefficient (r) of mean summer $dust_T$ at Izaña with the NAFDI from 1987 to 2012 (r = 0.75, Fig. 1a) indicates that the dust export is highly sensitive to the dipole intensity (Fig. 3a).

The NAFD influences the spatial distribution of dust over the North Atlantic. To illustrate this we determined the metric Major Dust Activity Frequency (MDAF): the number of days with AI values > 1 divided by the total number of (August) days in %. The mean wind fields and precipitation rates are also shown along with MDAF for low and high NAFDI summers in Fig. 2.

Increases in the NAFDI are associated with a strengthening of the zonal (easterly) component of trade winds north of the ITCZ in a region we define as the subtropical Saharan Stripe (Fig. 2c and d). This strengthening of easterly winds was observed in all standard levels (only shown at 925 and 700 hPa for the sake of brevity). The subtropical Saharan Stripe region, which extends from Central Algeria to Western Saharan between 24 and 30° N, includes important dust sources (Prospero et al., 2002; Schepanski et al., 2009; Rodríguez et al., 2011; Ginoux et al., 2012) which clearly exhibit a greater MDAF during summers with high NAFDI (Fig. 2b2). Long term (1987–2012) NAFDI and $dust_T$ at Izaña are highly correlated with the zonal wind in the subtropical Saharan Stripe (r = 0.85 and 0.65, see Fig. 4a and the Supplement, respectively). These correlations reflect the net result of a wide range of dust related processes (emission, vertical transport, advection to the Atlantic and size dependent deposition during transport).

The portion of the SAL with a high MDAF during more than 40 % of the summertime extends from North Africa to 30° W during summers with a low NAFDI (Fig. 2b1); in contrast the region extends to 55° W during high NAFDI summers (Fig. 2b2). In high NAFDI summers the SAL also expands northward over the subtropical North Atlantic domain (24–35° N, 9–60° W; Fig. 2b); because of this, the MDAF over the subtropical North Atlantic shows a significant correlation with the NAFDI (1979–2012 r = 0.74; Fig. 5). The positive correlation of NAFDI with the MDAF in the North Atlantic subtropical band (24–35° N, Fig. 4b) evidences how summer to summer variability in zonal

ACPD
14, 26689–26719, 2014

CC BY

winds in the subtropical Saharan Stripe (Figs. 2a and 4a) influences on dust export at subtropical latitudes. Reinforcement of easterly winds during high NAFDI summers is also observed in the AEJ (Fig. 2d), which plays a role in the trans-Atlantic dust transport (Jones et al., 2003).

4.3 Long term variability of dust size distribution

Our dust record in two size fractions was used to assess long term variability in dust size distribution. We found that the NAFD is correlated with the interannual variability of dust size distribution. Our measurements show pronounced changes in the size distribution of dust particles that are apparently related to wind interannual variability driven by the NAFDI (Fig. 3b). Dust tends to be coarser during high NAFDI years than during low NAFDI years. Observe how the $\text{dust}_{2.5}$ to dust_{T} ratio tends to decrease with the NAFDI increase: $\sim 35\,\%$ in summers with a NAFDI < 0 and down to $\sim 20\,\%$ in summers with a NAFDI > 1 (Fig. 3b). The high amount of coarse (> 2.5 µm) dust during high NAFDI summers may be linked to the activation of dust sources closer to the Atlantic coast and/or faster atmospheric transport due to higher wind speeds. Both processes will reduce the loss rate of larger-size particles due to gravitational deposition during transport (Ryder et al., 2013).

4.4 Connection of NAFD to climate variability

In this section we assess if the NAFDI could be used for linking long term export of Saharan dust with climate variability during the last decades. Here we present some associations between NAFDI, tropical rains and ENSO that will require future investigations.

South of the ITCZ, NAFD is associated with the variability in the tropical monsoon rains. We found that from 1987 to 2012 the interannual variability of the NAFDI is correlated with the precipitation rates over tropical North Africa (Fig. 4c) and with what we defined the Wet Sahel Portion ($r = 0.54$, Fig. 1b), i.e. the portion of the Sahel region

ACPD
14, 26689–26719, 2014

CC BY

(14–18° N to 17° W–22° E; Fig. 2e) that experienced a precipitation rate $\geq 3\,\mathrm{mm\,d^{-1}}$. This suggests that NAFD may also influence Sahelian dust emissions and consequently dust impacts in the tropical North Atlantic (Prospero and Lamb, 2003). The low MDAF in the Sahel and in the tropical rain band during high NAFDI summers supports this (Fig. 2b2). The association of NAFDI with the monsoon rains (Fig. 4c) and the implications for dust emissions and scavenging, accounts for the negative correlation of NAFDI with the MDAF over the Sahel and tropical North Africa (Fig. 4b), in a region where rainfall and mixing between the inland monsoon flow and the SAL may influence on spatial and temporal distribution of dust (Canut et al., 2010). The long term (1987–2012) correlation of $\mathrm{dust_T}$ at Izaña with the Wet Sahel Portion ($r = 0.74$, Fig. 1b) suggests that the NAFD influences climate variability throughout western North Africa. This modulation of dust export and monsoon rains by the NAFDI may account for the results obtained by Wilcox et al. (2010), who found that tropical rainfall rain band shifted northward by 1 to 4° latitude during dust outbreak events accompanied by an acceleration of winds in the northern edge of the EAJ.

We also compared the NAFDI with a set of teleconnection indexes and found that the Multivariate ENSO (El Niño Southern Oscillation) Index (MEI), – calculated with sea level pressure, zonal and meridional components of the surface wind, sea surface temperature, surface air temperature and total cloudiness fraction of the sky over the tropical Pacific Ocean – is moderately correlated with the NAFDI ($r = -0.50$) and with $\mathrm{dust_T}$ at Izaña (−0.59) (Fig. 1a) (see Supplement). This suggests that variability in MEI and in the NAFDI may be connected to global climate oscillations in the subtropics, e.g. intensity in the global trade winds belt, as also suggested by the correlation between NAFDI and the zonal component of trade winds (Fig. 4a). Intense ENSO years were clearly associated with low $\mathrm{dust_T}$ at Izaña, whereas intense La Niña periods were associated with high $\mathrm{dust_T}$ summers (Fig. 1a). Deficits in the North African tropical rains have been linked to ENSO (Folland et al., 1986), consistent with the correlation found between NAFDI and precipitation rates over tropical North Africa (Fig. 4c). Interannual variability in dust transport in subtropical Asia (Abish and Mohanakumar, 2013) and

CC BY

dust mobilization in sources affected by land use and ephemeral lakes (Ginoux et al., 2012) has also been linked to ENSO.

The increase in dust concentrations recorded in the tropical North Atlantic at Barbados (13°10′ N, 59°30′ W) since the mid 1970s has been linked to Sahelian droughts (Prospero and Lamb, 2003). Have similar changes occurred at subtropical Saharan latutudes? To address this issue we assumed that the "$dust_T$ vs. NAFDI relationship found for the period 1987–2012 period" is also valid for preceding decades, and used regression equation shown in Fig. 3a for estimating summer $dust_T$ at Izaña using the NAFDI from 1950 to 2012. We estimate persistent high dust concentrations (68 to 120 $\mu g\,m^{-3}$) at Izaña's subtropical latitude (Fig. 1c) from the mid-1950s to mid-1960s and relatively low dust concentrations from mid-1970s to mid-1980s (16 to 81 $\mu g\,m^{-3}$) (Fig. 1c). This NAFDI-based record at Izaña is markedly different from that based on measurements in Barbados which showed low dust concentrations prior to the onset of Sahelian drought in the early 1970s and high concentrations since then (Prospero and Lamb, 2003). This suggests that multidecadal changes in the NAFDI may have modulated the latitudinal transport pathways of North African dust across the Atlantic. This is supported by our overall results which show that high values of the NAFDI enhance dust transport at subtropical latitudes and rainfall in the Sahel (Fig. 4).

5 Conclusions

In this study, we have focused on identifying the relationship between long term interannual variability in Saharan dust export and large scale meteorology in western North Africa in summer. For this purpose, we analysed ∼ 25 year (1987–2012) dust concentrations recorded at the high altitude Izaña observatory (2373 m a.s.l.) in Tenerife Island, satellite and meteorological NCEP/NCAR reanalysis data.

Because Saharan dust export occurs at altitudes 1–5 km we paid special attention to the summer meteorological scenario at the 700 hPa standard level, which we so-called North African dipole, formed by an anticyclone over the subtropical Sahara and

CC BY

lower pressures over the tropics. We measured the variability of this summer scenario by the North AFrican Dipole Index (NAFDI): the difference of the 700 hPa geopotential heights anomalies averaged over central Morocco (subtropic) and over Bamako region (tropic). Variability in the NAFDI has meteorological implications throughout western North Africa.

We show that long term (multidecadal) interannual variability of summer meteorology as represented by the NAFDI influences on dust export from North Africa, transport pathways and dust size distribution. Increases in the NAFDI enhance Saharan dust export at subtropical latitudes due to the NAFDI is correlated (i) with increases in zonal wind speeds (at all standard levels, surface to 500 hPa) at the north of the Inter-Tropical Convergence Zone (Harmattan winds), and (ii) with monsoon rainfalls over the tropical North Africa and the Sahel. These correlations we found between processes occurring at distant regions evidence the interconnections between the different pieces that constitute the complex meteorological puzzle of the summer meteorological scenario in western North Africa (e.g. subtropical North African high, Saharan heat low, monsoon, African Easterly Jet, among others).

Our results suggest that the NAFDI driven long term variability in Saharan dust export may be influenced by global oscillations in the climate of tropics and subtropics (e.g. intensity of trade wind belt), as represented by the ENSO.

Here we have presented connections between Saharan dust export and large scale meteorology. Further studies will be necessary for understanding how long term interannual variability of the NAFDI may influence on the frequency and intensity of dust emission mechanisms (e.g. low-level jets, "haboob" storms or microscale dust devils and dusty plumes among others) and dust regional distribution processes (e.g. upward transport linked to convergence, mesoscale dry convective systems, among others).

The Supplement related to this article is available online at doi:10.5194/acpd-14-26689-2014-supplement.

cc BY

Acknowledgements. This study is a result of the project POLLINDUST (CGL2011-26259), funded by the Minister of Economy and Competitiveness of Spain. The Izaña GAW program is funded by AEMET. We gratefully acknowledge the cooperation of the NOAA/ESRL Physical Sciences Division, the NASA Goddard Earth Science data and Information Services Center and the NOAA Air Resources Laboratory. JMP research is supported by NSF grant AGS-0962256. MIG holds a grant from the Canarian Agency for Research, Innovation and Information Society and the European Social Fund. We thank our colleague Celia Milford for the comments and suggestions that improved the original manuscript.

References

Abish, B. and Mohanakumar, K.: Absorbing aerosol variability over the Indian subcontinent and its increasing dependence on ENS O, Global Planet. Change, 106, 13–19, 2013. 26703

Adams, A. M., Prospero, J. M., and Zhang, C.: CALIPSO-derived three-dimensional structure of aerosol over the Atlantic Basin and adjacent continents, J. Climate, 25, 6862–6879, doi:10.1175/JCLI-D-11-00672.1, 2012. 26691, 26693

Allen, C. J. T. and Washington, R.: The low-level jet dust emission mechanism in the central Sahara: observations from Bordj-Badji Mokhtar during the June 2011 fennec intensive observation period, J. Geophys. Res.-Atmos., 119, 2990–3015, doi:10.1002/2013JD020594, 2013. 26698

Andrey, J., Cuevas, E., Parrondo, M. C., Alonso-Pérez, S., Redondas, A., and Gil-Ojeda, M.: Quantification of ozone reductions within the Saharan air layer through a 13-year climatologic analysis of ozone profiles, Atmos. Environ., 84, 28–34, 2014. 26698

Ashpole, I. and Washington, R.: Intraseasonal variability and atmospheric controls on daily dust occurrence frequency over the central and western Sahara during the boreal summer, J. Geophys. Res.-Atmos., 118, 12915–12926, doi:10.1002/2013JD020267, 2013. 26692, 26698

Baker, A. R. and Jickells, T. D.: Mineral particle size as a control on aerosol iron solubility, Geophys. Res. Lett., 33, L17608, doi:10.1029/2006GL026557, 2006. 26691

Ben-Ami, Y., Koren, I., and Altaratz, O.: Patterns of North African dust transport over the Atlantic: winter vs. summer, based on CALIPSO first year data, Atmos. Chem. Phys., 9, 7867–7875, doi:10.5194/acp-9-7867-2009, 2009. 26699

CC BY

Canut, G., Lothon, M., Saïd, F., and Lohou, F.: Observation of entrainment at the interface between monsoon flow and the Saharan Air Layer, Q. J. Roy. Meteor. Soc., 136, 34–46, 2010. 26698, 26703

Chiapello, I., Moulin, C., and Prospero, J. M.: Understanding the long-term variability of African dust transport across the Atlantic as recorded in both Barbados surface concentrations and large-scale Total Ozone Mapping Spectrometer (TOMS) optical thickness, J. Geophys. Res., 110, D18S10, doi:10.1029/2004JD005132, 2005. 26692

Cowie, S. M., Knippertz, P., and Marsham, J. H.: A climatology of dust emission events from northern Africa using long-term surface observations, Atmos. Chem. Phys., 14, 8579–8597, doi:10.5194/acp-14-8579-2014, 2014. 26698

Creamean, J. M., Suski, K. J., Rosenfeld, D., Cazorla, A., DeMott, P. J., Sullivan, R. C., White, A. B., Ralph, F. M., Minnis, P., Comstock, J. M., Tomlinson, J. M., and Prather, K.: Dust and biological aerosols from the Sahara and Asia influence precipitation in the western US, Science, 339, 1572–1578, doi:10.1126/science.1227279, 2013. 26691

Cuesta, J., Marsham, J. H., Parker, D. J., and Flamant, C.: Dynamical mechanisms controlling the vertical redistribution of dust and the thermodynamic structure of the West Saharan atmospheric boundary layer during summer, Atmos. Sci. Lett., 10, 34–42, doi:10.1002/asl.207, 2009. 26698

Cuevas, E., Camino, C., Benedetti, A., Basart, S., Terradellas, E., Baldasano, J. M., Morcrette, J. J., Marticorena, B., Goloub, P., Mortier, A., Berjón, A., Hernández, Y., Gil-Ojeda, M., and Schulz, M.: The MACC-II 2007–2008 reanalysis: atmospheric dust evaluation and characterization over northern africa and middle east, Atmos. Chem. Phys. Discuss., submitted, 2014. 26699

Delmonte, B., Petit, J. R., Andersen, K. K., Basile-Doelsch, I., Maggi, V., and Lipenkov, V. Y.: Dust size evidence for opposite regional atmospheric circulation changes over east Antarctica during the last climatic transition, Clim. Dynam., 23, 427–438, doi:10.1007/s00382-004-0450-9, 2004. 26691

Díaz, J., Tobías, A., and Linares, C.: Saharan dust and association between particulate matter and case-specific mortality: a case-crossover analysis in Madrid (Spain), Environ. Health, 11, 11, doi:10.1186/1476-069X-11-11, 2012. 26691

Draxler, R. R. and Rolph, G. D.: HYSPLIT (HYbrid Single-Particle Lagrangian Integrated Trajectory) Model access via NOAA ARL READY Website, available at: http://ready.arl.noaa.gov/

CC BY

HYSPLI~T.php (last access: March 2014), NOAA Air Resources Laboratory, Silver Spring, MD, USA, 2013. 26696
Engelstaedter, S. and Washington, R.: Atmospheric controls on the annual cycle of North African dust, J. Geophys. Res., 112, D17111, doi:10.1029/2006JD007195, 2007. 26692, 26698
Fiedler, S., Schepanski, K., Heinold, B., Knippertz, P., and Tegen, I.: Climatology of nocturnal lowlevel jets over North Africa and implications for modeling mineral dust emission, J. Geophys. Res.-Atmos., 118, 6100–6121, doi:10.1002/jgrd.50394, 2013. 26698
Flamant, C., Chaboureau, J. P., Parker, D. J., Taylor, C. M., Cammas, J. P., Bock, O., Timouk, F., and Pelon, J.: Airborne observations of the impact of a convective system on the 10 planetary boundary layer thermodynamics and aerosol distribution in the inter-tropical discontinuity region of the West African Monsoon, Q. J. Roy. Meteor. Soc., 133, 1175–1189, doi:10.1002/qj.97, 2007. 26697, 26698
Folland, C. K., Palmer, T. N., and Parker, D. E.: Sahel rainfall and worldwide sea temperatures, 1901–85, Nature, 320, 602–607, doi:10.1038/320602a0, 1986. 26703
Font-Tullot, I.: Las invasiones de aire caliente africano en el Archipiélago Canario, Revista de Geofísica, IX, 36, 334–349, 1950. 26698, 26699
Forster, P., Ramaswamy, V., Artaxo, P., Berntsen, T., Betts, R., Fahey, D. W., Haywood, J., Lean, J., Lowe, D. C., Myhre, G., Nganga, J., Prinn, R., Raga, G., Schulz, M., and Van Dorland, R.: Climate Change 2007: The Physical Science Basis, Contribution of Working Group I to the Fourth Assessment Report of the Intergovernmental Panel on Climate Change, chap. Changes, in: Atmospheric Constituents and in Radiative Forcing, Cambridge University Press, Cambridge, UK and New York, NY, USA, 659–740, 2007. 26691
Ginoux, P., Prospero, J. M., Torres, O., and Chin, M.: Long-term simulation of global dust distribution with the GOCART model: correlation with North Atlantic Oscillation, Environ. Modell. Softw., 19, 113–128, 2004. 26691, 26692
Ginoux, P., Prospero, J. M., Gill, T. E., Hsu, N. C., and Zhao, M.: Global-scale attribution of anthropogenic and natural dust sources and their emission rates based on MODIS Deep Blue aerosol products, Rev. Geophys., 50, RG3005, doi:10.1029/2012RG000388, 2012. 26691, 26692, 26701, 26704
Guirado, C., Cuevas, E., Cachorro, V. E., Toledano, C., Alonso-Pérez, S., Bustos, J. J., Basart, S., Romero, P. M., Camino, C., Mimouni, M., Zeudmi, L., Goloub, P., Baldasano, J. M., and de Frutos, A. M.: Aerosol characterization at the Saharan AERONET site Tamanrasset,

ACPD
14, 26689–26719, 2014

Atmos. Chem. Phys. Discuss., 14, 16641–16690, doi:10.5194/acpd-14-16641-2014, 2014. 26698

Haywood, J. M., Pelon, J., Formenti, P., Bharmal, N., Brooks, M., Capes, G., Chazette, P., Chou, C., Christopher, S., Coe, H., Cuesta, J., Derimian, Y., Desboeufs, K., Greed, G., Harrison, M., Heese, B., Highwood, E. J., Johnson, B., Mallet, M., Marticorena, B., Marsham, J., Milton, S., Myhre, G., Osborne, S. R., Parker, D. J., Rajot, J. L., Schulz, M., Slingo, A., Tanré, D., and Tulet, P.: Overview of the dust and biomass-burning experiment and African monsoon multidisciplinary analysis special observing period-0, J. Geophys. Res., 113, D00C17, doi:10.1029/2008JD010077, 2008. 26692

Herman, J. R., Bhartia, P. K., Torres, O., Hsu, C., Seftor, C., and Celarier, E.: Global distribution of UV-absorbing aerosols from Nimbus 7/TOMS data, J. Geophys. Res., 102, 16911–16922, doi:10.1029/96JD03680, 1997. 26693

Hosseinpour, F. and Wilcox, E. M.: Aerosol interactions with African/Atlantic climate dynamics, Environ. Res. Lett., 9, 075004, doi:10.1088/1748-9326/9/7/075004, 2014. 26699

Huneeus, N., Schulz, M., Balkanski, Y., Griesfeller, J., Prospero, J., Kinne, S., Bauer, S., Boucher, O., Chin, M., Dentener, F., Diehl, T., Easter, R., Fillmore, D., Ghan, S., Ginoux, P., Grini, A., Horowitz, L., Koch, D., Krol, M. C., Landing, W., Liu, X., Mahowald, N., Miller, R., Morcrette, J.-J., Myhre, G., Penner, J., Perlwitz, J., Stier, P., Takemura, T., and Zender, C. S.: Global dust model intercomparison in AeroCom phase I, Atmos. Chem. Phys., 11, 7781–7816, doi:10.5194/acp-11-7781-2011, 2011. 26691

Immler, F. and Schrems, O.: Vertical profiles, optical and microphysical properties of Saharan dust layers determined by a ship-borne lidar, Atmos. Chem. Phys., 3, 1353–1364, doi:10.5194/acp-3-1353-2003, 2003. 26698, 26699

Jickells, T. D., An, Z. S., Andersen, K. K., Baker, A. R., Bergametti, G., Brooks, N., Cao, J. J., Boyd, P. W., Duce, R. A., Hunter, K. A., Kawahata, H., Kubilay, N., laRoche, J., Liss, P. S., Mahowald, N., Prospero, J. M., Ridgwell, A. J., Tegen, I., and Torres, R.: Global iron connections between desert dust, ocean biogeochemistry and climate, Science, 308, 67–71, doi:10.1126/science.1105959, 2005. 26691

Jones, C., Mahowald, N., and Luo, C.: The role of easterly waves on African desert dust transport, J. Climate, 16, 3617–3628, 2003. 26697, 26698, 26702

Kalnay, E., Kanamitsu, M., Kistler, R., Collins, W., Deaven, D., Gandin, L., Iredell, M., Saha, S., White, G., Woollen, J., Zhu, Y., Leetmaa, A., Reynolds, R., Chelliah, M., Ebisuzaki, W., Higgins, W., Janowiak, J., Mo, K. C., Ropelewski, C., Wang, J., Jenne, R., and Joseph, D.: The

CC BY

NCEP/NCAR 40-Year Reanalysis Project, B. Am. Meteorol. Soc., 77, 437–471, 1996. 26693, 26696

Karyampudi, V., Palm, S., Reagen, J., Fang, H., Grant, W., Hoff, R., Moulin, C., Pierce, H., Torres, O., Browell, E., and Melfi, S.: Validation of the saharan dust plume conceptual model using lidar, Meteosat, and ECMWF data, B. Am. Meteorol. Soc., 80, 1045–1075, 1999. 26698

Knippertz, P.: Dust emissions in the West African heat trough – the role of the diurnal cycle and of extratropical disturbances, Meteorol. Z., 17, 553–563, 2008. 26698

Knippertz, P. and Todd, M. C.: The central west Saharan dust hot spot and its relation to African easterly waves and extratropical disturbances, J. Geophys. Res., 115, D12117, doi:10.1029/2009JD012819, 2010. 26692, 26697, 26698

Knippertz, P. and Todd, M. C.: Mineral dust aerosols over the Sahara: meteorological controls on emission and transport and implications for modeling, Rev. Geophys., 50, RG1007, doi:10.1029/2011RG000362, 2012. 26692, 26698

Lafore, J. P., Flamant, C., Giraud, V., Guichard, F., Knippertz, P., Mahfouf, J. F., Mascart, P., and Williams, E. R.: Introduction to the AMMA Special Issue on "Advances in understanding atmospheric processes over West Africa through the AMMA field campaign", Q. J. R. Meteor. Soc., 136, 2–7, 2010. 26697, 26698

Lau, K. M., Kim, K. M., Sud, Y. C., and Walker, G. K.: A GCM study of the response of the atmospheric water cycle of West Africa and the Atlantic to Saharan dust radiative forcing, Ann. Geophys., 27, 4023–4037, doi:10.5194/angeo-27-4023-2009, 2009. 26699

Li, J., Carlson, B. E., and Lacis, A. A.: A study on the temporal and spatial variability of absorbing aerosols using Total Ozone Mapping Spectrometer and Ozone Monitoring Instrument Aerosol Index data, J. Geophys. Res., 114, D09213, doi:10.1029/2008JD011278, 2009. 26696

Lavaysse, C., Flamant, C., Janicot, S., Parker, D. J., Lafore, J.-P., Sultan, B., and Pelon, J.: Seasonal evolution of the West African heat low: a climatological perspective, Clim. Dynam., 33, 313–330, doi:10.1007/s00382-009-0553-4, 2009. 26697

Lavaysse, C., Flamant, C., and Janicot, S.: Regional-scale convection patterns during strong and weak phases of the Saharan heat low, Atmos. Sci. Lett., 11, 255–264, doi:10.1002/asl.284, 2010a. 26698

Lavaysse, C., Flamant, C., Janicot, S., and Knippertz, P.: Links between African easterly waves, midlatitude circulation and intraseasonal pulsations of the West African heat low, Q. J. R. Meteor. Soc., 136, 141–158, doi:10.1002/qj.555, 2010b. 26698

Mahowald, N., Albani, S., Kok, J. F., Engelstaeder, S., Scanza, R., Ward, D. S., and Flanner, M. G.: The size distribution of desert dust aerosols and its impact on the Earth system, Aeolian Res., 15, 53–71, doi:10.1016/j.aeolia.2013.09.002, 2014. 26691, 26699

Mallone, S., Stafoggia, M., Faustini, A., Gobbi, J. P., Marconi, A., and Forastiere, F.: Saharan dust and associations between particulate matter and daily mortality in Rome, Italy, Environ. Health Persp., 119, 1409–1414, doi:10.1289/ehp.1003026, 2011. 26691

Marsham, J., Parker, D., Grams, C., Taylor, C., and Haywood, J.: Uplift of Saharan dust south of the intertropical discontinuity, J. Geophys. Res., 113, D21102, doi:10.1029/2008JD009844, 2008. 26698

Marticorena, B., Chatenet, B., Rajot, J. L., Traoré, S., Coulibaly, M., Diallo, A., Koné, I., Maman, A., NDiaye, T., and Zakou, A.: Temporal variability of mineral dust concentrations over West Africa: analyses of a pluriannual monitoring from the AMMA Sahelian Dust Transect, Atmos. Chem. Phys., 10, 8899–8915, doi:10.5194/acp-10-8899-2010, 2010. 26692

Martínez-García, A., Rosell-Melé, A., Geibert, W., Gersonde, R., Masqué, P., Gaspari, V., and Barbante, C.: Links between iron supply, marine productivity, sea surface temperature, and CO_2 over the last 1.1 Ma, Paleoceanography, 24, PA1207, doi:10.1029/2008PA001657, 2009. 26691

Menut, L., Chiapello, I., and Moulin, C.: Predictability of mineral dust concentrations: the African monsoon multidisciplinary analysis first short observation period forecasted with CHIMERE-DUST, J. Geophys. Res., 114, D07202, doi:10.1029/2008JD010523, 2009. 26692

Mulitza, S., Heslop, D., Pittauerova, D., Fischer, H. W., Meyer, I., Stuut, J. B., Zabel, M., Mollenhauer, G., Collins, J. A., Kuhnert, H., and Schulz, M.: Increase in African dust flux at the onset of commercial agriculture in the Sahel region, Nature, 466, 226–228, doi:10.1038/nature09213, 2010. 26692

Nicholson, S. E.: A revised picture of the structure of the "monsoon" and land ITCZ over West Africa, Clim. Dyn., 32, 1155–1171, doi:10.1007/s00382-008-0514-3, 2009. 26696, 26697, 26698

Nicholson, S. E.: The West African Sahel: A Review of Recent Studies on the Rainfall Regime and Its Interannual Variability, ISRN-Meteorology, 2013, 453521, 32, doi:10.1155/2013/453521, 2013. 26693, 26697, 26698, 26699

Otto, S., de Reus, M., Trautmann, T., Thomas, A., Wendisch, M., and Borrmann, S.: Atmospheric radiative effects of an in situ measured Saharan dust plume and the role of large particles, Atmos. Chem. Phys., 7, 4887–4903, doi:10.5194/acp-7-4887-2007, 2007. 26691

CC BY

Pérez, L., Tobías, A., Querol, X., Künzli, N., Pey, J., Alastuey, A., Viana, M., Valero, N., González-Cabré, M., and Sunyer, J.: Coarse particles from Saharan dust and daily mortality, Epidemiology, 19, 800–807, doi:10.1097/EDE.0b013e31818131cf, 2008. 26691

Pérez García-Pando, C., Stanton, M. C., Diggle, P. J., Trzaska, S., Miller, R. L., Perlwitz, J. P., Baldasano, J. M., Cuevas, E., Ceccato, P., Yaka, P., and Thomson, M. C.: Soil dust aerosols and wind as predictors of seasonal meningitis incidence in Niger, Environ. Health. Persp., Environ. Health Perspect., 122, 679–686, doi:10.1289/ehp.1306640, 2014. 26691

Pospichal, B., Karam, D. B., Crewell, S., Flamantb, C., Hünerbein, A., Bock, O., and Saïde, F.: Diurnal cycle of the intertropical discontinuity over West Africa analysed by remote sensing and mesoscale modelling, Q. J. R. Meteorol. Soc., 136, 92–106, 2010. 26697

Prospero, J. M. and Carlson, T. N.: Vertical and areal distribution of Saharan dust over the western Equatorial North Atlantic Ocean, J. Geophys. Res., 77, 5255–5265, 1972. 26698, 26699

Prospero, J. M. and Lamb, P. J.: African droughts and dust transport to the Caribbean: climate change implications, Science, 302, 1024–1027, doi:10.1126/science.1089915, 2003. 26692, 26699, 26703, 26704

Prospero, J. M., Ginoux, P., Torres, O., Nicholson, S. E., and Gill, T. E.: Environmental characterization of global sources of atmospheric soil dust identified with the Nimbus 7 Total Ozone Mapping Spectrometer (TOMS) absorbing aerosol product, Rev. Geophys., 40, 2-1–2-31, doi:10.1029/2000RG000095, 2002. 26695, 26701, 26716

Prospero, J. M., Collard, F. X., Molinié, J., and Jeannot, A.: Characterizing the annual cycle of African dust transport to the Caribbean Basin and South America and its impact on the environment and air quality, Global Biogeochem. Cy., 29, 757–773, doi:10.1002/2013GB004802, 2014. 26691

Ridley, D. A., Heald, C. L., and Prospero, J. M.: What controls the recent changes in African mineral dust aerosol across the Atlantic?, Atmos. Chem. Phys., 14, 5735–5747, doi:10.5194/acp-14-5735-2014, 2014. 26692

Rodríguez, S., Querol, X., Alastuey, A., Kallos, G., and Kakaliagou, O.: Saharan dust contributions to PM_{10} and TSP levels in Southern and Eastern Spain, Atmos. Environ., 35, 2433–2447, doi:10.1016/S1352-2310(00)00496-9, 2001. 26691

Rodríguez, S., González, Y., Cuevas, E., Ramos, R., Romero, P. M., Abreu-Afonso, J., and Redondas, A.: Atmospheric nanoparticle observations in the low free troposphere during

CC BY

upward orographic flows at Izaña Mountain Observatory, Atmos. Chem. Phys., 9, 6319–6335, doi:10.5194/acp-9-6319-2009, 2009. 26694

Rodríguez, S., Alastuey, A., Alonso-Pérez, S., Querol, X., Cuevas, E., Abreu-Afonso, J., Viana, M., Pérez, N., Pandolfi, M., and de la Rosa, J.: Transport of desert dust mixed with North African industrial pollutants in the subtropical Saharan Air Layer, Atmos. Chem. Phys., 11, 6663–6685, doi:10.5194/acp-11-6663-2011, 2011. 26694, 26701

Rodríguez, S., Alastuey, A., and Querol, X.: A review of methods for long term in situ characterization of aerosol dust, Aeolian Res., 6, 55–74, doi:10.1016/j.aeolia.2012.07.004, 2012. 26694, 26695

Ryder, C. L., Highwood, E. J., Lai, T. M., Sodemann, H., and Marsham, J. H.: Impact of atmospheric transport on the evolution of microphysical and optical properties of Saharan dust, Geophys. Res. Lett., 40, 2433–2438, doi:10.1002/grl.50482, 2013. 26691, 26702

Schepanski, K., Tegen, I., Todd, M. C., Heinold, B., Bönisch, G., Laurent, B., and Macke, A.: Meteorological processes forcing Saharan dust emission inferred from MSG-SEVIRI observations of subdaily dust source activation and numerical models, J. Geophys. Res., 114, D10201, doi:10.1029/2008JD010325, 2009. 26701

Spengler, T. and Smith, R. K.: The dynamics of heat lows over flat terrain, Q. J. R. Meteor. Soc., 134, 2157–2172, 2008. 26697

Tanaka T. Y. and Chiba M.: A numerical study of the contribution of dust source regions to the global dust budget, Global Planet. Change, 52, 88–104, 2006. 26691, 26692

Tesche, M., Ansmann, A., Muller, D., Althausen, D., Mattis, I., Heese, B., Freudenthaler, V., Wiegner, M., Esselborn, M., Pisani, G., and Knippertz, P.: Vertical profiling of saharan dust with Raman lidars and airborne HSRL in southern Morocco during SAMUM, Tellus B, 61, 144–164, doi:10.1111/j.1600-0889.2008.00390.x, 2009. 26699

Tsamalis, C., Chédin, A., Pelon, J., and Capelle, V.: The seasonal vertical distribution of the Saharan Air Layer and its modulation by the wind, Atmos. Chem. Phys., 13, 11235-11257, doi:10.5194/acp-13-11235-2013, 2013. 26693, 26696, 26698, 26699

Welti, A., Lüönd, F., Stetzer, O. and Lohmann, U.: Influence of particle size on the ice nucleating ability of mineral dusts, Atmos. Chem. Phys., 9, 6705–6715, doi:10.5194/acp-9-6705-2009, 2009. 26691

Wilcox, E. M., Lau, K. M., and Kim, K.-M.: A northward shift of the North Atlantic Ocean Intertropical Convergence Zone in response to summertime Saharan dust outbreaks, Geophys. Res. Lett., 37, L04804, doi:10.1029/2009GL041774, 2010. 26703

ACPD
14, 26689–26719, 2014

Modulation of Saharan dust export by the North African dipole

S. Rodríguez et al.

CC BY

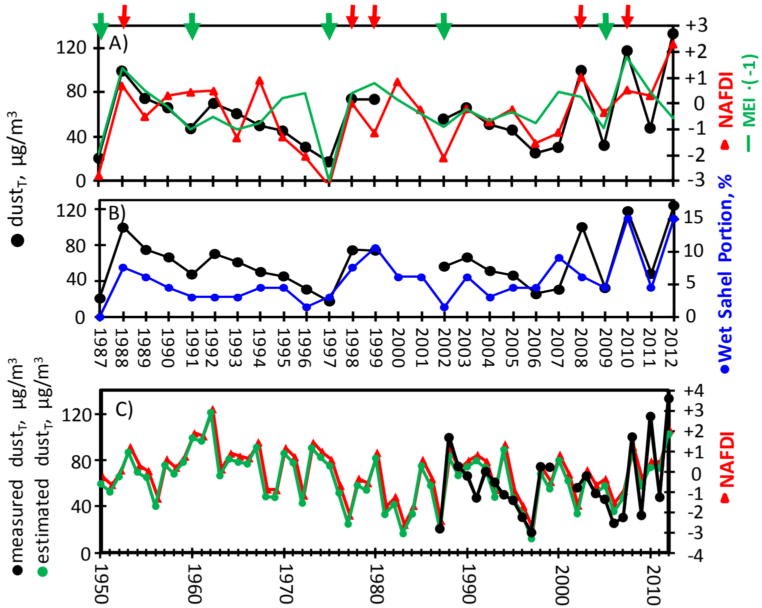

Figure 1. Long term evolution of summer dust and climate indexes. **(A, B)** Concentrations of $dust_T$ measured at Izaña (black dot) and the MEI (green line), NAFDI (red triangle) and Wet Sahel Portion (blue dot) indexes from 1987 to 2012. Green and red arrows highlight moderate and intense ENSO and La Niña summers, respectively (http://www.cpc.ncep.noaa.gov). **(C)** NAFDI and measured and estimated $dust_T$ concentrations at Izaña between 1950 and 2012.

ACPD
14, 26689–26719, 2014

Modulation of Saharan dust export by the North African dipole

S. Rodríguez et al.

CC BY

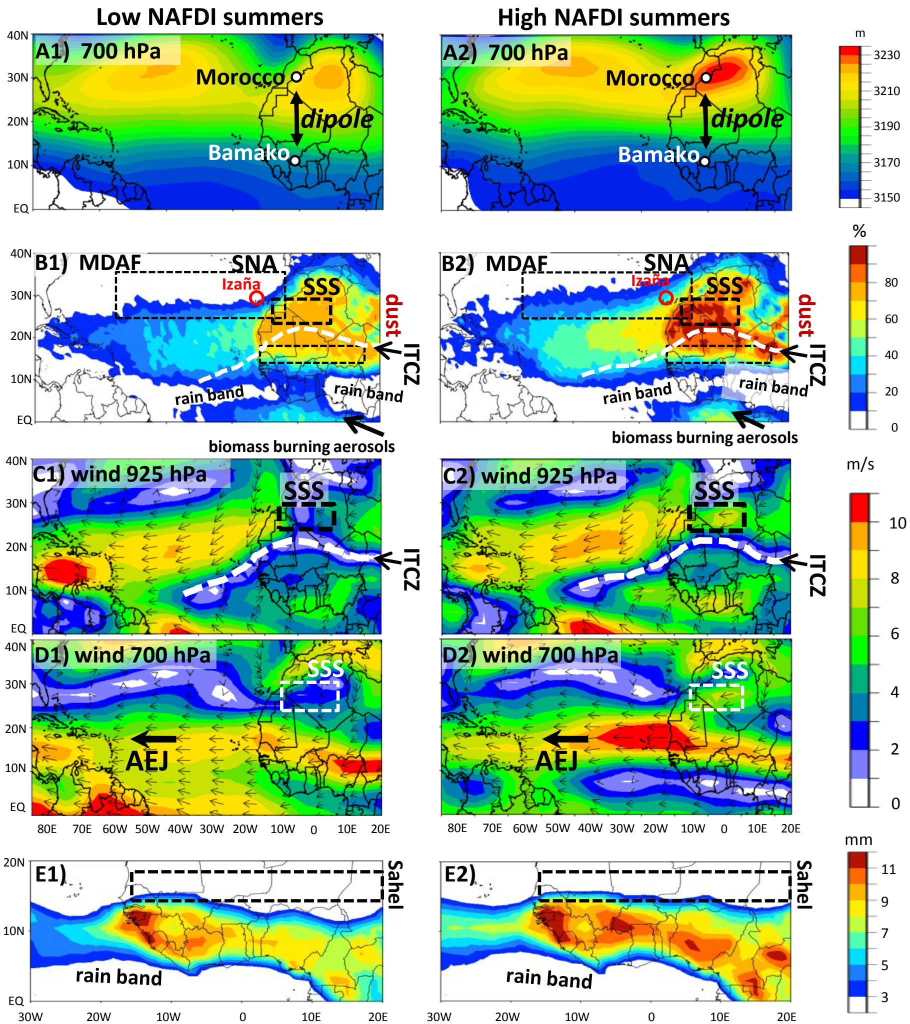

ACPD
14, 26689–26719, 2014

Modulation of Saharan dust export by the North African dipole

S. Rodríguez et al.

CC BY

Figure 2. North African dipole and spatial distribution of dust and meteorological fields averaged in low and high NAFDI summers. High NAFDI summers represents the average of the three highest NAFDI recorded in the 1987–2012 period (1988, 2008 and 2012 = +1.0, +1.2, +2.1, respectively). Low NAFDI summers represents the average of the three lowest NAFDI recorded in the 1987–2012 period (1987, 1996 and 1997 = −2.4, −1.7 and −2.9, respectively). **(A)** Height of 700 hPa geopotential highlighting the location of the two regions used for determining the NAFDI. **(B)** MDAF at the north of the rain band (data at the south of the tropical rain band is due to biomass burning aerosols from Southern Africa) (Prospero et al., 2002). Mean winds at **(C)** 925 hPa (≈ 800 m a.s.l.) and **(D)** 700 hPa (≈ 3000 m a.s.l.). **(E)** Mean precipitation rates. The location of the Inter-Tropical Convergence Zone (ITCZ), the Subtropical Saharan Stripe (SSS), the African Easterly Jet (AEJ) and the Subtropical North Atlantic (SNA) are highlighted.

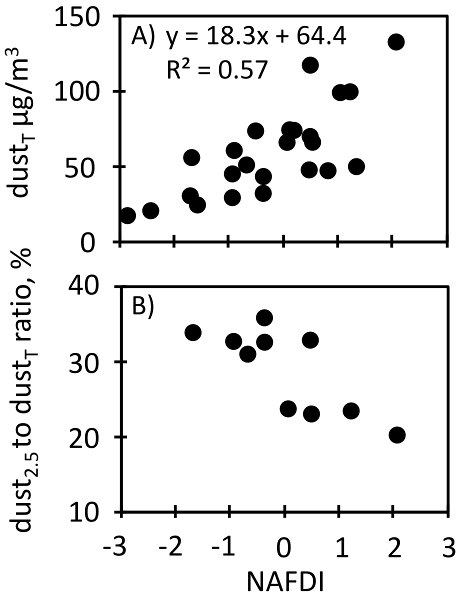

Figure 3. Scatter plot of total dust and fine-to-total dust ratio vs. NAFDI index. **(A)** Summer mean $dust_T$ at Izaña vs. NAFDI (1987–2012). **(B)** Summer mean $dust_{2.5}$-to-$dust_T$ ratio vs. NAFDI (2002–2012).

ACPD
14, 26689–26719, 2014

Modulation of Saharan dust export by the North African dipole

S. Rodríguez et al.

CC BY

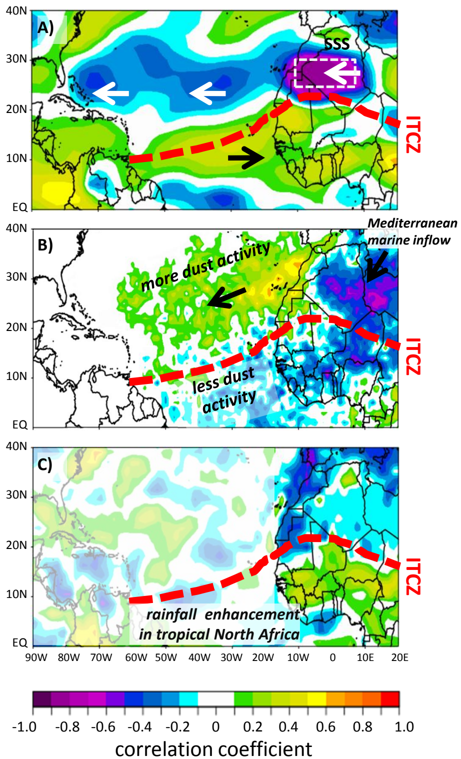

Figure 4. Influence of the NAFD strengthening on zonal winds, spatial distribution of dust and precipitation rate. Correlation coefficient between long term (1987–2012) summer NAFDI and **(A)** zonal wind **(B)** MDAF and **(C)** precipitation rate. The Inter-Tropical Convergence Zone (ITCZ) and the Subtropical Saharan Stripe (SSS) are highlighted. Arrows indicate **(A)** zonal wind direction and **(B)** relevant airflows for dust mobilization.

ACPD
14, 26689–26719, 2014

CC BY

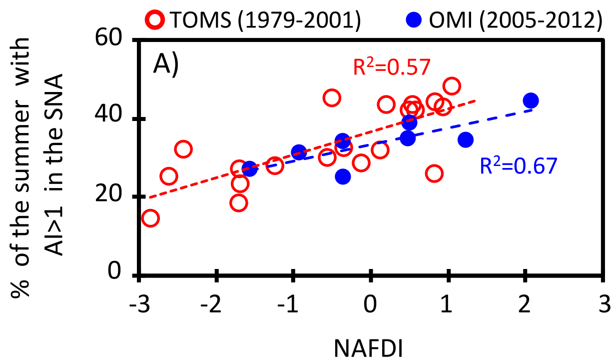

Figure 5. Scatter plot of summer dust activity in the subtropical North Atlantic vs. the NAFDI. MDAF in the Subtropical North Atlantic (SNA) vs. the NAFDI. Measurements of the TOMS (red circle) and OMI (blue dot) satellite borne sensors were used. The R^2 coefficient of the linear fitting is included.

ACPD
14, 26689–26719, 2014

CC BY